Available online at www.sciencedirect.com
SCIENCE DIRECT®
Biochemical Pharmacology 66 (2003) 447–458
Biochemical Pharmacology
www.elsevier.com/locate/biochempharm

The anti-neoplastic and novel topoisomerase II-mediated cytotoxicity of neoamphimedine, a marine pyridoacridine

Kathryn M. Marshall[a], Sandra S. Matsumoto[a], Joseph A. Holden[b], Gisela P. Concepción[d], Deniz Tasdemir[c], Chris M. Ireland[c], Louis R. Barrows[a,*]

[a]*Department of Pharmacology and Toxicology, 30 S. 2000 E. Rm. 201, Salt Lake City, UT 84112, USA*
[b]*Department of Pathology, University of Utah, Salt Lake City, UT, USA*
[c]*Department of Medicinal Chemistry, University of Utah, Salt Lake City, UT, USA*
[d]*Marine Science Institute, University of the Philippines, Diliman, Quezon City, Philippines*

Received 17 June 2002; accepted 27 January 2003

Abstract

Topoisomerase IIα (top2) is a target of some of the most useful anticancer drugs. All clinically approved top2 drugs act to stabilize a drug–enzyme–DNA cleavable complex. Here we report the novel top2 activity of neoamphimedine, an isomer of the marine pyridoacridine amphimedine. Neoamphimedine was cytotoxic in yeast and mammalian cell lines. Neoamphimedine exhibited enhanced toxicity in top2 over-expressing yeast cells and was toxic in every mammalian cell line tested. However, neoamphimedine did not possess enhanced toxicity in a mammalian cell line sensitive to stabilized cleavable complexes. Therefore, we hypothesized that neoamphimedine is a top2-dependent drug, whose primary mechanism of action is not the stabilization of cleavable complexes. Top2-directed activity was determined in purified enzyme systems. Neoamphimedine-induced catenation of plasmid DNA only in the presence of active top2. This catenation correlated with the ability of neoamphimedine to aggregate DNA. Catenation was also observed using a filter-binding assay and transmission electron microscopy. Catenation was confirmed when only restriction enzyme digestion could resolve the catenated plasmid complex to monomer length plasmid DNA. Neoamphimedine also showed potent anti-neoplastic activity in human xenograft tumors in athymic mice. Neoamphimedine was as effective as etoposide in mice bearing KB tumors and as effective as 9-aminocamptothecin in mice bearing HCT-116 tumors. Amphimedine did not induce DNA aggregation or catenation *in vitro*, nor did it display any significant anti-neoplastic activity. These results suggest that neoamphimedine has a novel top2-mediated mechanism of cytotoxicity and anticancer potential.

Keywords: Neoamphimedine; Amphimedine; Marine pyridoacridine; DNA catenation; Topoisomerase II

1. Introduction

Top2 is an essential ubiquitous enzyme. It facilitates relaxation of supercoiled DNA and decatenation of plasmid DNA *in vitro*. Top2 is a proven anti-neoplastic target and classic top2 drugs comprise an important class of chemotherapeutic agents that all share a basic mechanism of action, stabilizing top2–DNA "cleavable complexes" [1,2]. Stabilized cleavable complexes are processed into DNA double strand breaks and are lethal to the cell. Top2 drugs include doxorubicin, duanorubicin, etoposide, and many others used to treat human solid tumors and hematologic malignancies [3].

Neoamphimedine is a recently discovered top2 active pyridoacridine that was isolated from *Xestospongia* sp. sponges collected in the Philippines and Micronesia [4]. Amphimedine, a regioisomer of neoamphimedine, was the first pyridoacridine described in a class that now numbers over 40. The precise mechanism of cytotoxicity varies amongst the pyridoacridines, however, DNA-directed activity is considered a major contributing mechanism of

* Corresponding author. Tel.: +1-801-581-4547; fax: +1-801-585-5111.
E-mail address: lbarrows@deans.pharm.utah.edu (L.R. Barrows).

Abbreviations: top2, topoisomerase IIα; IC_{50}, 50% inhibitory concentration of the drug; DMSO, dimethyl sulfoxide; PAGE, poly-acrylamide gel electrophoresis; TEM, transmission electron microscopy; α-MEM, Minimal Essential Medium alpha modification; MTT, (3-(4,5-dimethylthiazol-2-yl)-2,5-diphenyltetrazolium bromide); HMW, high molecular weight; SDS, sodium dodecyl sulfate; PVA, polyvinyl alcohol; rf, circular double-strand replicative form; T/C, average increase in tumor volume of treated animals divided by the average increase in tumor volume of control animals; SE, standard error.

0006-2952/$ – see front matter © 2003 Published by Elsevier Science Inc.
doi:10.1016/S0006-2952(03)00209-0

action [5–7]. This activity is suggested by their planar structures and supported by various studies [5,6,8,9].

This paper evaluates the cytotoxicity of neoamphimedine in yeast cells expressing normal and elevated top2 levels and reports IC_{50} values for several mammalian cell lines. Evidence for the unique *in vitro* activity of neoamphimedine, induction of top2-mediated plasmid DNA catenation, is presented. This activity has previously been reported for molecules that cause DNA compaction [10,11]. It is not shared by amphimedine nor any of the other pyridoacridines tested. In addition, the antitumor activity of neoamphimedine and amphimedine were compared *in vivo*. Neoamphimedine has excellent antitumor activity in animal models, an activity not shared by amphimedine.

2. Materials and methods

2.1. Reagents

Isolation and chemical characterization of neoamphimedine has been described [4]. Amphimedine and neoamphimedine were isolated from a *Xestospongia* sp. sponge from the Philippines (Fig. 1). Drug standards were purchased from Sigma Chemical Co. Radioactive thymidine was purchased from New England Nuclear. Restriction enzymes and buffers were purchased from New England Biolabs. All other chemicals were purchased from Sigma Chemical Co. or Baker Chemical Co. Radiolabeled (4.4×10^3 cpm/g) ^{3}H replicative form (rf) of M13 mp19 was isolated by the alkaline lysis method as described in [12,13].

2.2. Yeast strains and plasmids

Rad 52− yeast strains JN394 and JN394T2 (contains YCpPDED1T2 plasmid that constitutively over-expresses yeast top2) and Rad 52+ yeast strains JN362a and the YCpPDED1T2 plasmid that constitutively over-expresses yeast top2 were generously provided by Dr. John L. Nitiss (St. Jude Children's Hospital, TN) [14,15]. Strain JN362a was transfected with YCpPDED1T2 using the lithium acetate method [16], to generate JN362aT2. Yeast strain BCY 123, a protease-deficient ura3 strain, was kindly supplied by Dr. Janet E. Lindsley (University of Utah). Plasmid YEpWOb6, which contains the human *top2α* gene under control of a galactose promoter, was kindly supplied by Dr. James C. Wang (Harvard University, MA). Plasmid YEpWOb6 was transfected into yeast strain BCY 123 by the lithium acetate method [16]. Transformants were selected for by plating on minimal plates containing glucose (2%) and lacking uracil.

2.3. Top2 sensitivity assay in yeast

Yeast strains JN394 and JN362a were grown in rich medium containing 20 mg/mL glucose. Yeast strains JN394T2 and JN362aT2 were grown in minimal medium lacking uracil but containing 20 mg/mL glucose (pH 5.5–6.0), 1.5 mg/mL yeast nitrogen base without amino acids and ammonium sulfate (DIFCO), 5 mg/mL ammonium sulfate and amino acids. Cells were grown overnight and counted with a hemocytometer. Cells were diluted to 10^6 in media, drug dissolved in 100% DMSO was added and cells were grown for 24 hr. Control yeast cells were treated with an equal amount of DMSO used in drug treatment, which did not exceed 1% of the cell media. After 24 hr, cells were plated in duplicate or triplicate onto rich agarose plates to determine clonal survival. Percent clonal survival was calculated by normalizing all counts so the control (DMSO-treated) cell counts equaled 100%.

2.4. Isolation of human top2 from yeast

Human top2α was induced and isolated from yeast strain BCY 123, containing plasmid YEpWOb6 as described in [13]. Enzymatic activity was determined by assaying for decatenation of kinetoplast DNA [17]. The purified 170 kDa species of top2 was identified by denaturing PAGE analysis [11].

2.5. Quantitation of DNA catenation and cleavage

DNA cleavage assays were performed as described in [13]. In brief, 20 μL volumes containing 50 mM Tris–HCl

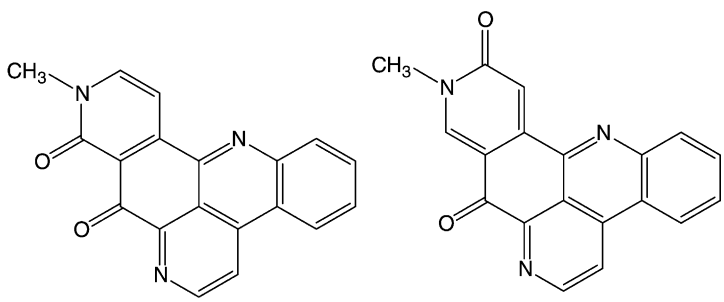

Neoamphimedine Amphimedine

Fig. 1. Structures of neoamphimedine and amphimedine.

(pH 7.5), 85 mM KCl, 10 mM $MgCl_2$, 0.5 mM EDTA, 30 μg/mL bovine serum albumin, 2 mM DTT, 500 ng of radiolabeled and supercoiled rf M13 mp19 DNA and 80–120 ng purified top2 (unless otherwise noted) were treated with drug (in DMSO) and incubated at 30° for 30 min. The reactions were stopped by the addition of 2 μL of 1.5 mg/mL proteinase K in 0.5% SDS and incubated at 37° for 60 min. The DNA was fractionated by electrophoresis in 0.8% agarose (containing 50 ng ethidium bromide/mL TAE) to separate catenated, nicked, cut, relaxed and supercoiled DNA. DNA was visualized under UV light and sliced out of the gel. Gel slices were placed in scintillation vials with 1 mL water, melted in a microwave oven and mixed with 10 mL Opti-Fluor (Packer Co.) while molten, and radioactivity determined by standard liquid scintillation counting. The percentage of cleaved DNA, represented by radioactivity in the combined nicked and linear bands, was determined relative to the total radioactivity in the reactions, following subtraction of radioactivity due to endogenously cleaved DNA. The percentage of catenated DNA was determined similarly.

2.6. Isolation and restriction enzyme digestion of top2-treated DNA

DNA from the above cleavage reactions was electroeluted from the agarose gel following the method of Ausubel *et al.* [18]. Equal volumes (22 μL) of phenol and chloroform:isoamyl alcohol (24:1) were added to the reacted DNA. This mixture was centrifuged for 15 min at 13,000 *g* in a bench top microfuge. The aqueous phase was transferred to a second microfuge tube, containing 13 μL 99% ice-cold ethanol, 1 μL 5 M NaCl and 0.5 μL 2 M $MgCl_2$. The DNA was precipitated by freezing for 15 min followed by centrifugation at 4° for 15 min at 13,000 *g*. The ethanol was aspirated, 13 μL of ice-cold 70% ethanol was added with mixing, followed by freezing for 5 min and centrifugation at 4° for 5 min at 13,000 *g*. The ethanol was again aspirated and DNA allowed to air dry.

High molecular weight DNA isolated from top2 reactions with neoamphimedine underwent restriction digestion to assess whether the high molecular weight complexes consisted of catenated plasmid. This was carried out using a restriction digest method described previously [19]. Distilled H_2O (18 μL) was added to each tube of DNA, along with 2 μL restriction enzyme NE Buffer 3 (50 mM Tris–HCl, 10 mM $MgCl_2$, 100 mM NaCl, 1 mM DTT), and 1 μL restriction enzyme *Sal* I (10 u/μL). The reaction mixture was incubated at 37° for 3 hr before electrophoretic fractionation on a 0.8% agarose gel.

2.7. Transmission electron microscopy analysis of catenated DNA

TEM allows molecular interactions to be magnified up to 200,000×. A Hitachi H-7100 transmission electron microscope with lab-6 filament was used. DNA catenated by reaction with neoamphimedine and top2 in the cleavage assay was electroeluted from the agarose gel and applied to formvar-coated grids for TEM viewing. This was carried out using the protocol described by Thresher and Griffith [20]. To attach DNA to the TEM grids, the grids were floated on 10 μL electroeluted DNA in HNE solution buffer (20 mM HEPES (pH 7.3), 30 mM NaCl, 0.1 mM EDTA) for 5 min. Next, the grids were floated on 4% filtered glutaraldehyde solution in HNE buffer for 10 min to fix the DNA, followed by positive staining with a saturated aqueous uranyl acetate solution for 10 min. The grids were washed with distilled water and allowed to dry. Equal amounts of DNA from neoamphimedine treated or untreated reactions were applied to the grids. Once DNA was attached to the grid, the grid was inserted into the TEM and analyzed. Areas of DNA attachment to the grid were located under low magnitude and then resolved in more detail at higher magnification, 20,000–70,000× magnification was used to view the DNA samples.

2.8. Cell culture

The human colon tumor cell line (HCT-116), human epidermoid-nasopharyngeal tumor cell line (KB), human melanoma cell line (SK-mel-5), human breast cancer cell line (MCF7), human ovarian cell lines (A2780 and A2780AD), and Chinese hamster ovary (CHO) cell lines: AA8 (wild type), and xrs-6 (double strand break repair-deficient) were used. HCT-116, KB, SK-mel-5, MCF7 and AA8 cell lines were purchased from ATCC. A2780 and A2780AD cell lines were provided by Dr. Jindrich Kopecek (University of Utah) and the xrs-6 cell line was a generous gift from Dr. Penny A. Jeggo and co-workers (University of Sussex, UK). AA8, xrs-6, and KB cells were maintained in α-MEM supplemented with 10% bovine fetal and calf sera (Atlanta Biologicals), 100 u/mL penicillin and 100 μg/mL streptomycin. HCT-116 cells were maintained in McCoy's medium similarly enriched with 2% fetal bovine serum, 8% newborn bovine serum with 100 u/mL penicillin, 100 μg/mL streptomycin. Cells were grown at 37° as monolayers in 75-cm^2 culture flasks and detached with trypsin before seeding into microtiter culture plates.

2.9. Cell cytotoxicity

Cytotoxicity was established in an MTT assay as performed by Mosmann [21] and modified by others [22–24]. Drugs were dissolved in 100% DMSO at initial concentrations of 10 mM and serially diluted. The final concentration of DMSO in the cell culture wells was 1% or less. Cells were seeded in 200 μL of growth media in Corning 96-well microtiter plates at 30,000 cells per well (AA8), 40,000 cells per well (xrs-6), or 20,000 cells per well (human cell lines). Four hours after seeding, cells were

treated, each dose in quadruplicate, with 2 μL of drug (CHO cell lines) or 1 μL of drug (all other cell lines). CHO cell lines were refed at 18 hr. After 72 hr, all cultures were refed with 100 μL McCoy's medium and 11 μL MTT (5 mg/mL in PBS, pH 7.4) was added to each well. The plates were incubated for 4 hr at 37°. Viable cells reduced MTT to a purple formazan product that was solubilized by the addition of 100 μL DMSO to aspirated culture wells. The absorbance at 540 nm was measured for each well using a Bio-Rad MP450 plate reader. Average absorbance for each set of drug-treated wells was compared to the average absorbance of the control wells to determine the fractional survival at any particular drug concentration. The inhibitory concentration 50 (IC_{50}) was defined as the drug concentration that yielded a fractional survival of 50%. IC_{50} values reported were the average of three to five independent experiments.

2.10. DNA filter-binding assay

HMW DNA complexes were quantified using a filter-binding assay [25]. In brief, catenated-radiolabeled DNA was detected when 100 μL of SDS wash (40 mM Tris (pH 7.5), 500 mM NaCl, 25 mM EDTA and 1% SDS) was added to top2 reaction mixtures, after 30 min of incubation at 30°, and passed through 0.45 μm HA nitrocellulose membrane filters (Millipore) attached to a vacuum. The filter was then washed with 3 mL of the SDS wash. SDS wash denatured HMW DNA (aggregated DNA), trapping only catenated DNA on the filter. The filter was then completely dried before being placed in 10 mL Opti-Fluor and counted in a liquid scintillation counter. DNA aggregation was quantifiable in this system when TE (40 mM Tris, pH 7.5, 25 mM EDTA) wash was used instead of SDS wash. TE wash allowed HMW DNA complexes to bind to the filter as both aggregated and catenated DNA. All monomer plasmid DNA still passed through the filter. Total DNA was determined by adding control reaction mixtures to a nitrocellulose filter without filtering. Filtering and washing the appropriate control DNA mixtures determined background counts. DNA counts determined in filtered reactions were divided by the counts determined in non-filtered reactions, and multiplied by 100%, after subtracting background counts.

2.11. In vivo studies

KB or HCT-116 cells (2×10^6) were injected into the flanks of nude (BalbC nu/nu) mice. The KB animals were randomized when the tumors were staged at 50 mm^3 volume and were treated with the first of three i.p. injections, 4qd. Doses were 50 mg/kg etoposide, amphimedine, or neoamphimedine. Animals bearing HCT-116 tumors were randomized similarly and dosed with four i.p. injections, 4qd. HCT-116 animals were treated with 12.5, 25, and 50 mg/kg neoamphimedine and 1 mg/kg 9-aminocamptothecin. Drugs were administered in 0.02% α-methylcarboxy-cellulose α-MEM. Control animals were injected with vehicle. All groups contained 5 mice, except control, which had 10 mice. Animals were excluded from analysis if their tumor volume at staging was less than 45 mm^3 or if tumor volume exceeded 300 mm^3. IACUC approval #UU 00-05004.

3. Results

3.1. Enhanced toxicity of neoamphimedine in yeast that overproduce top2

Neoamphimedine and amphimedine were tested for cytotoxicity in Rad 52+/− yeast strains expressing normal or elevated top2 levels. The strains used were top2 normal JN394 and JN362a, and top2 over-expressing, JN394T2 and JN362aT2 [15]. Etoposide served as a positive control and topotecan as a negative control in this experiment. Etoposide (Fig. 2a) and neoamphimedine (Fig. 2b) showed enhanced toxicity in the Rad 52− strains and in the top2 over-expressing strains. Neither topotecan, a top1 poison, nor amphimedine showed enhanced toxicity in the Rad 52−, top2 over-expressing yeast (data not shown).

3.2. Cytotoxicity of neoamphimedine in mammalian cells

Neoamphimedine was cytotoxic in every mammalian cell line examined, while amphimedine did not show toxicity at tested doses (Table 1). Neoamphimedine retained its cytotoxicity in the MDR-expressing A2780AD cell line, while doxorubicin (33-fold), M-AMSA (8-fold), and taxol (15-fold) all had significantly reduced toxicity compared to the A2780 wild type cell line. In addition, because a top2-dependent mechanism of cell killing was suggested by the yeast assay, both neoamphimedine and amphimedine were tested in a panel of mutant CHO cell lines. These lines lack various pathways of DNA repair. Top2 poisons

Table 1
Cell cytotoxicity assay

	IC_{50} (μM)	
	Neoamphimedine	Amphimedine
HCT-116	4.5	>50
SK-mel-5	7.6	>50
KB	6.0	>50
MCF7	1.8	>50
A2780wt	0.9	>50
A2780AD	0.83	>50
AA8	2.5	>100
xrs-6	1.6	>100

IC_{50} values in μM of neoamphimedine and amphimedine determined using the MTT-microtiter plate assay. Values are the average of three to five independent experiments.

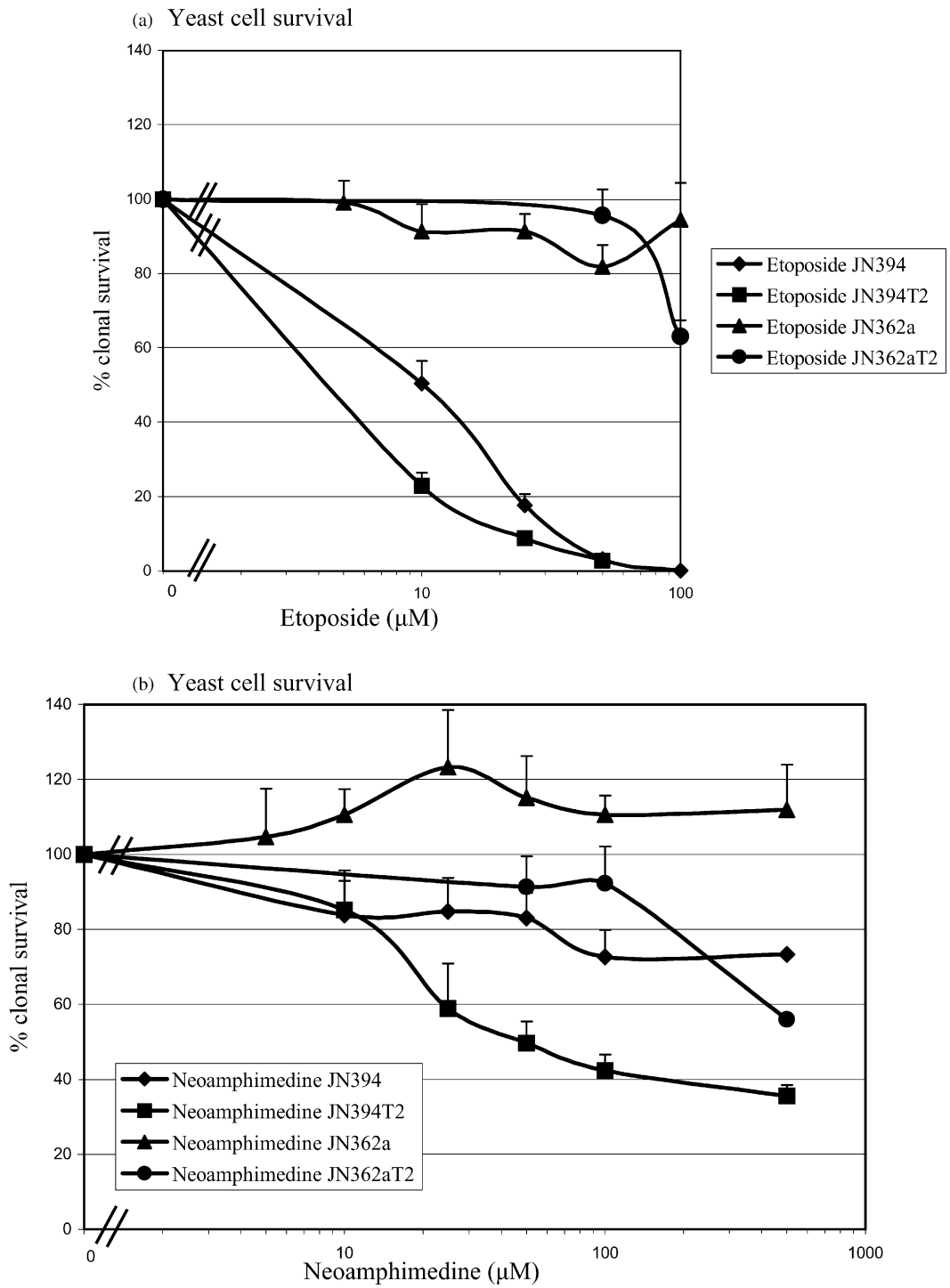

Fig. 2. Cytotoxicity of etoposide and neoamphimedine in yeast. Etoposide was tested at 5, 10, 25, 50 and 100 μM in yeast cell lines JN394 (Rad 52−), JN394T2 (Rad 52−, top2 over-expresser), JN362a (Rad 52+) and JN362aT2 (Rad 52+, top2 over-expresser) (a). Neoamphimedine was tested at 5, 10, 25, 50, 100 and 500 μM in yeast cell lines JN394 (Rad 52−), JN394T2 (Rad 52−, top2 over-expresser), JN362a (Rad 52+) and JN362aT2 (Rad 52+, top2 over-expresser) (b). Both etoposide and neoamphimedine displayed enhanced toxicity in the Rad 52− and top2 over-expressing strains. Values are means ± standard error, $N \geq 3$. The data points were simply connected by smoothed lines.

that stabilize cleavable complexes are exceptionally toxic to the xrs-6 [23] cells, which are deficient in ku 80 and therefore lack DNA double strand break repair. No significant enhancement of cytotoxicity was detected at IC_{50} for neoamphimedine or amphimedine in the xrs-6 cells, although a small increase was observed in the xrs-6 cell line treated with neoamphimedine compared to the AA8 cell line. This result appeared inconsistent with the yeast data [15], because all the clinical top2 drugs tested in the xrs-6 cell line have shown significantly enhanced toxicity

Table 2
Quantification of drug-dependent top2 plasmid catenation and cleavage

	84 ng top2[a]		140 ng top2	
	Percent catenated	Percent cleaved	Percent catenated	Percent cleaved
DNA only	0	0	0	0
DNA + top2	0	0	0	0
DNA + top2 + 100 μM etop[b]	≤0	25.5 ± 4.1[c]	≤0	24.7 ± 1.9
DNA + top2 + 1 μM neo	≤0	≤0[d]	1.7 ± 1.3	≤0
DNA + top2 + 2.5 μM neo	≤0	3.5 ± 2.5	3.7 ± 1.2	≤0
DNA + top2 + 5 μM neo	≤0	≤0	2.0 ± 0.6	≤0
DNA + top2 + 10 μM neo	≤0	1.7 ± 1.3	1.3 ± 1.5	≤0
DNA + top2 + 25 μM neo	4.0 ± 1	≤0	4.0 ± 1.5	≤0
DNA + top2 + 50 μM neo	3.2 ± 1.4	8.9 ± 2.1	8.7 ± 4.3	≤0
DNA + top2 + 75 μM neo	4.1 ± 1.1	6.0 ± 2.4	19.7 ± 7.9	≤0
DNA + top2 + 100 μM neo	11.1 ± 3.7	4.8 ± 3.4	18.0 ± 8.0	≤0
DNA + top2 + 200 μM neo	9.9 ± 2.5	0.2 ± 2.2	24.3 ± 8.8	≤0
DNA + top2 + 300 μM neo	16.3 ± 2.9	1.1 ± 2.5	17.6 ± 5.1	≤0
DNA + top2 + 400 μM neo	15.2 ± 1.6	1.1 ± 3.8	26.7 ± 13.2	≤0
DNA + top2 + 500 μM neo	20.2 ± 1.2	4.6 ± 4.0	19.0 ± 4.0	≤0

[a] top2 concentrations are given as ng/22 μL reaction volume.
[b] etop, etoposide; neo, neoamphimedine.
[c] Values are means ± standard error, N ≥ 3.
[d] Electrophoresis lanes were loaded with equal amounts of DNA, as catenation occurred less total DNA remained in nicked or circular plasmid bands. When DNA of these bands were normalized to DNA control bands, the results were frequently slightly negative.

[23]. Therefore, it was hypothesized that neoamphimedine is a top2-dependent drug, whose primary mechanism of action is not the stabilization of cleavable complexes.

3.3. Neoamphimedine catenation of DNA in vitro

The ability of neoamphimedine to interfere with the function of purified human top2 was investigated *in vitro*. In top2–DNA cleavage assays, neoamphimedine-induced minimal DNA cleavage via formation of cleavage complexes. In experiments using 84 ng top2, up to 8.9% DNA cleavage (50 μM neoamphimedine) was detected. This percentage of cleavage decreased as neoamphimedine concentrations increased, and cleavage was not detected in experiments using 140 ng top2 (Table 2). Gel electrophoresis indicated that this cleavage was due to single strand DNA nicking of the plasmid substrate (Fig. 3a).

At the same time, an unexpected activity was revealed (Fig. 3a). In reactions containing active top2 and 91 μM neoamphimedine, the supercoiled substrate DNA routinely appeared as a HMW complex upon electrophoretic analysis. This activity was concentration-dependent and was apparent whether the substrate plasmid was relaxed (Fig. 4) or supercoiled. Table 2 shows the dependency of plasmid catenation, using 84 and 140 ng top2, on the concentration of neoamphimedine (1–500 μM). The amount of HMW DNA formed under this protocol appears to plateau at approximately 300 μM neoamphimedine. Table 3 shows the dependency of plasmid catenation, using 300 μM neoamphimedine, on the concentration of top2 (8–420 ng). The HMW complex formation was not observed with amphimedine nor any of the approximately 30 other

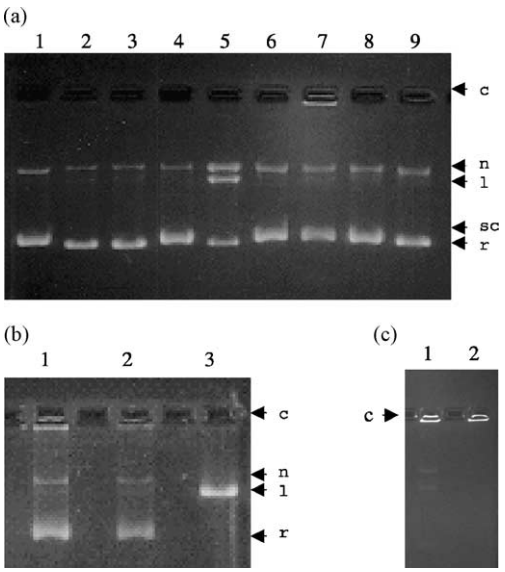

Fig. 3. HMW DNA, produced from supercoiled plasmid DNA, by active top2 in the presence of neoamphimedine (a) and *Sal* I digestion of the HMW DNA complex (b), HMW DNA produced using PVA (c). Cleavage gels resolved DNA as either catenated (c), nicked (n), linear (l), supercoiled (sc), or relaxed (r). Gel (a) contains the following in each well: (1) DNA only, (2) DNA + top2, (3) DNA + top2 + 20% DMSO, (4) DNA + 91 μM etoposide, (5) DNA + top 2 + 91 μM etoposide, (6) DNA + 91 μM neoamphimedine, (7) DNA + top2 + 91 μM neoamphimedine, (8) DNA + 91 μM amphimedine, (9) DNA + top2 + 91 μM amphimedine. HMW DNA was formed only in the presence of active top2 and neoamphimedine (see lane 7). Gel (b) contains the following in each well, from left to right: (1) DNA + top2 + 91 μM neoamphimedine, (2) DNA + top2 + 91 μM neoamphimedine + *Sal* I (inactivated), (3) DNA + top2 + 91 μM neoamphimedine + *Sal* I (active). The HMW DNA complex was broken only when restriction enzyme digestion cut catenated plasmids in one region, forming a linear band (see lane 3). Gel (c) contains the following in both lanes (1) and (2): DNA + top2 + 7.5% PVA.

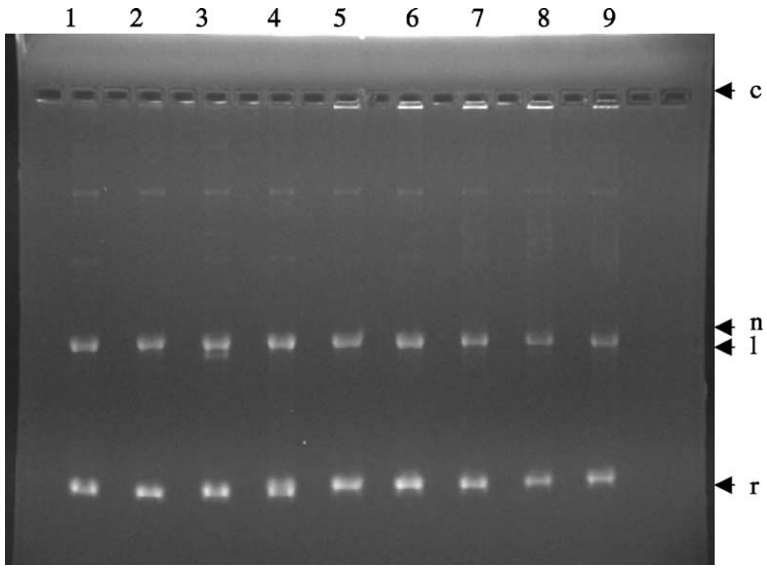

Fig. 4. Neoamphimedine catenation of relaxed DNA. Cleavage gel resolved DNA as either catenated (c), nicked (n), linear (l) or relaxed (r). There was no supercoiled DNA used in this experiment. Gel contains the following from left to right: (1) DNA only, (2) DNA + top2 + 20% DMSO, (3) DNA + top2 + 50 μM etoposide, (4) DNA + top2 + 50 μM neoamphimedine, (5) DNA + top2 + 100 μM neoamphimedine, (6) DNA + top2 + 200 μM neoamphimedine, (7) DNA + top2 + 300 μM neoamphimedine, (8) DNA + top2 + 400 μM neoamphimedine, and (9) DNA + top2 + 500 μM neoamphimedine.

pyridoacridines tested recently in our laboratory. The formation of the HMW DNA complex was dependent upon the presence of active top2 and neoamphimedine.

To determine if protein–DNA aggregation or chemical cross-linking were mechanisms causing the HMW DNA complex, the HMW DNA band was electroeluted from agarose gels and either: (a) subjected to extensive protease digestion followed by SDS treatment, (b) treated with SDS and boiling, or (c) treated with the restriction enzyme, *Sal* I (M13 mp19 has one *Sal* I site); all of which were followed by agarose gel electrophoresis. Only the *Sal* I treatment was able to disrupt the HMW DNA complex, in this case all the DNA resolved as a monomer length plasmid band (Fig. 3b). This result indicated that the HMW DNA was in fact a catenated complex of plasmid DNA.

Electroeluted HMW DNA formed in the presence of top2 and neoamphimedine, and monomer plasmid DNA isolated from top2 reactions not containing neoamphimedine, were prepared for TEM analysis. Equal amounts of DNA, imaged in 2-D, distinguished between catenated and monomer plasmid DNA. The HMW DNA was seen as a concentrated continuous-lattice of DNA. Monomer plasmid DNA appeared as dispersed smaller fragments of DNA (Fig. 5). Other than the size of the complexes, no difference between HMW and monomer plasmid DNA could be determined. Positive uranyl acetate staining of the plasmid DNA confirmed that DNA was imaged.

3.4. DNA catenation correlated with DNA aggregation

A DNA filter-binding assay was employed to quantify DNA catenation detected originally by gel electrophoresis. PVA has been shown to aggregate DNA, inducing top2 catenation [25]. Catenated DNA was retained on 0.45-μm

Table 3
Quantification of top2-dependent plasmid catenation and cleavage

	Control		Etoposide[a]		Neoamphimedine	
	Percent cat[b]	Percent cleaved	Percent cat	Percent cleaved	Percent cat	Percent cleaved
8 ng top2[c]	≤0	≤0[d]	0.5 ± 1.2[e]	≤0	2.8 ± 0.9	≤0
42 ng top2	≤0	≤0	≤0	6.5 ± 3.1	12.0 ± 2.5	5.8 ± 2.7
84 ng top2	≤0	≤0	≤0	25.5 ± 4.1	16.3 ± 2.9	1.1 ± 2.5
140 ng top2	≤0	2.3 ± 3.1	≤0	24.7 ± 1.9	17.6 ± 5.1	≤0
420 ng top2	3.3 ± 0.5	≤0	0.8 ± 0.8	28.0 ± 2.1	17.8 ± 3.2	≤0

[a] Drug concentrations: etoposide (100 μM), neoamphimedine (300 μM).
[b] cat, catenated plasmid DNA.
[c] top2 concentrations are given as ng/22 μL reaction volume.
[d] Electrophoresis lanes were loaded with equal amounts of DNA, as catenation occurred less total DNA remained in nicked or circular plasmid bands. When DNA of these bands were normalized to DNA control bands, the results were frequently slightly negative.
[e] Values are means ± standard error, N ≥ 3.

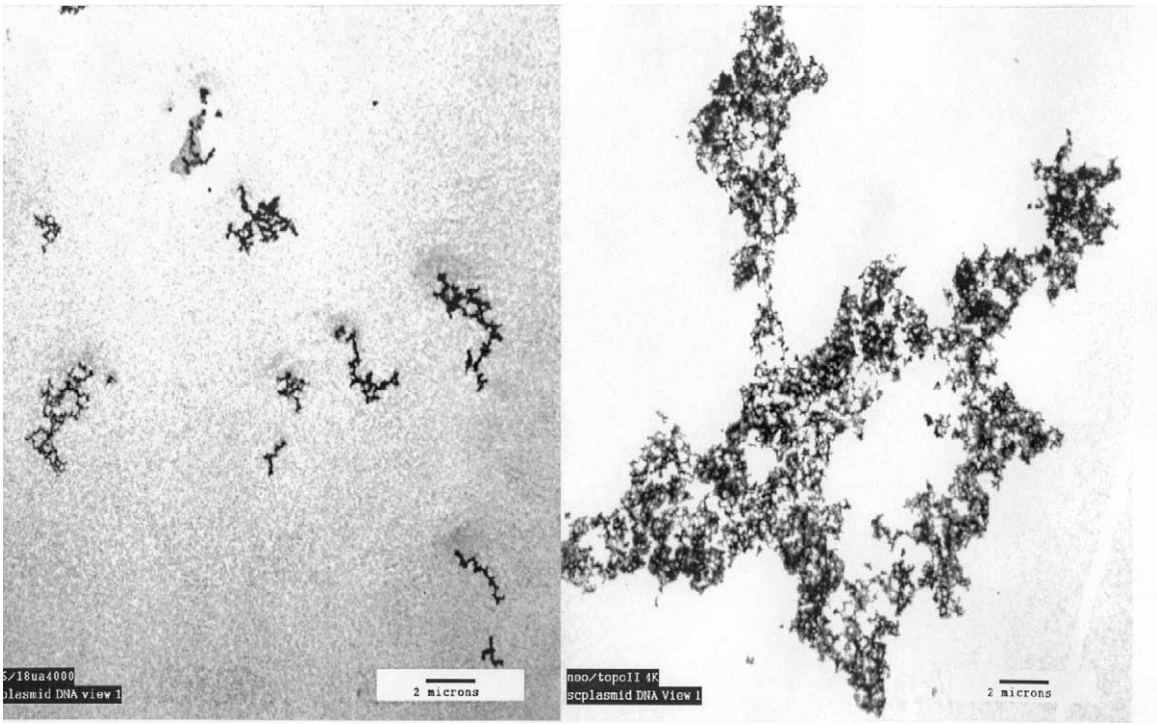

Fig. 5. Transmission electron microscopy of plasmid DNA. Transmission electron micrographs of monomer plasmid DNA + top2 (left) and HMW plasmid DNA + top2 + neoamphimedine DNA (right). HMW DNA complexes were observed as a concentrated continuous-lattice of DNA. These complexes are stable under denaturing conditions (heat and SDS) and when protease digested. Equal amounts of DNA were mounted on the grids prior to visualization.

membrane filters, while monomer plasmid DNA passed through in the presence of SDS wash.

In this assay, supercoiled plasmid DNA was used as substrate. After incubation of reactions, SDS or TE wash was added as described in Section 2. SDS wash denatured the DNA, breaking apart any aggregated DNA, capturing only catenated DNA on the filter. TE wash did not dissociate aggregated DNA, thus, the TE wash retained HMW DNA on the filter, both catenated and aggregated, allowing only monomer plasmid DNA to pass through. Results are illustrated in Fig. 6. Reactions were treated with increasing concentrations of neoamphimedine. Neoamphimedine reactions in the presence of active top2 aggregated DNA to a similar extent as neoamphimedine reactions in the absence of top2. When SDS wash was employed, neoamphimedine only formed catenated DNA in the presence of active top2. When inactive top2 (no ATP) was used in the reaction mix with neoamphimedine and washed with SDS, no DNA catenation was observed. Neoamphimedine was found to induce top2 to catenate DNA in a time- and concentration-dependent manner. Maximum catenation was attained at approximately 30 min under these conditions (160 ng top2). In the DNA filter-binding assay, catenated plasmid DNA reached a peak of 13% (±3.2%) at 300 μM neoamphimedine and then decreased at higher concentrations.

As mentioned, it was also possible to quantify DNA aggregation using the filter-binding assay. Aggregated DNA was stable in TE washes, and remained trapped on the filter. DNA aggregation was found to increase in proportion to the concentration of neoamphimedine (Fig. 6). Neoamphimedine was also able to aggregate linear and relaxed DNA (data not shown). Amphimedine failed to aggregate or catenate DNA in this system.

3.5. *In vivo* activity of neoamphimedine

Nude mice bearing human KB tumors in their flanks showed excellent anticancer activity for neoamphimedine. In this experiment, animals treated with vehicle, amphimedine, neoamphimedine, or etoposide were compared. Tumor growth in amphimedine-treated mice was not different from that of vehicle-treated mice. The best antitumor effects of neoamphimedine and etoposide were observed at the 50 mg/kg dose. Neoamphimedine showed statistically significant ($P < 0.05$) antitumor effects with a minimal T/C of 35% on day 8. Etoposide was also effective with a minimal T/C of 31% on day 15 ($P < 0.05$). Neoamphimedine was as effective as etoposide in this *in vivo* experiment. Amphimedine did not show any antitumor activity (Fig. 7a).

Neoamphimedine also showed antitumor activity in mice bearing HCT-116 cell tumors (Fig. 7b). Neoamphimedine was compared to 9-aminocamptothecin. Minimal T/C values of 36% on day 15 ($P < 0.05$, neoamphimedine 12.5 mg/kg), 30% on day 15 ($P < 0.05$, neoamphimedine 25 mg/kg), 36% on day 12 ($P < 0.05$, neoamphimedine 50 mg/kg), and 26% on day 15 ($P < 0.05$, 9-aminocamptothecin 1 mg/kg) were determined.

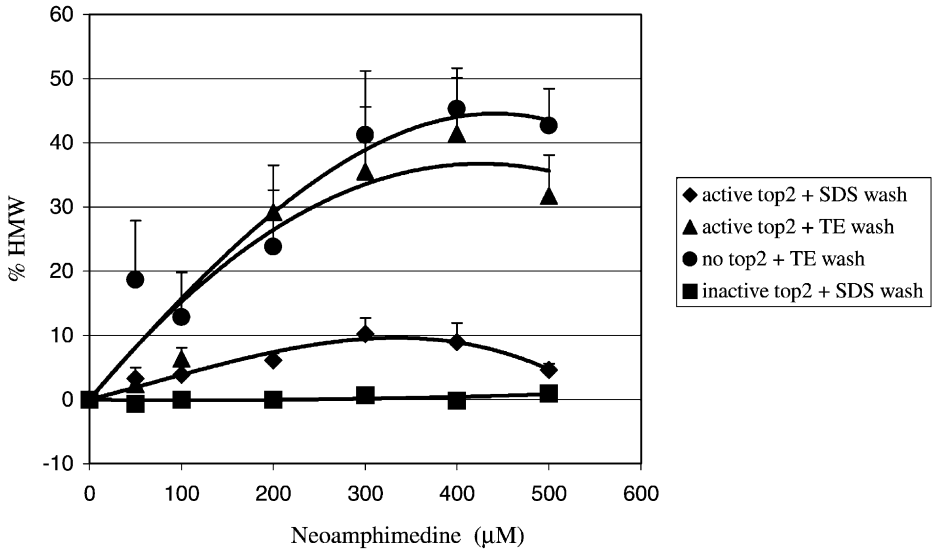

Fig. 6. DNA filter-binding assay. Catenated radiolabeled DNA was detected when SDS wash was added to the reaction mixture and passed through HA nitrocellulose membrane filters attached to a vacuum. SDS-wash denatures HMW DNA, trapping only catenated DNA on the filter. Aggregated DNA was detected when TE wash was used instead of SDS wash. TE wash allowed HMW complexes to bind to the filter as either aggregated or catenated DNA. DNA trapped on filters was quantified in a liquid scintillation counter. Amphimedine did not catenate nor aggregate plasmid DNA in the presence or absence of top2 (data not shown). Neoamphimedine also aggregated linear DNA (data not shown). Values are means ± standard error, $N \geq 6$. The data were fit to polynomial trend lines.

4. Discussion

Neoamphimedine is a unique top2 active drug, the structure of which was reported by de Guzman *et al.* [4]. This paper characterizes the activity of neoamphimedine in several systems. Yeast cell data indicated a top2-dependent mechanism of cytotoxicity that was Rad 52 sensitive. These data also demonstrate that the drug does not simply inhibit top2 activity. If depriving the cell of top2 were the mechanism of action for neoamphimedine, then yeast that over-express top2 (JN394T2) should be able to overcome drug-induced toxicity. We demonstrated that while neoamphimedine, like etoposide, has enhanced toxicity in the top2 over-expressing yeast, amphimedine toxicity was not influenced by top2 expression.

Because many top2 drugs act by stabilizing a DNA–drug–top2 cleavable complex, the toxicity of neoamphimedine was assessed in a CHO cell line that is super-sensitive to double strand DNA breaks [23]. Only minimal sensitivity of the xrs-6, compared to the repair competent AA8, was observed. Double strand DNA breaks are the principle cytotoxic lesion of drug stabilized top2 cleavable complexes [1]. However, drug inhibition of top2 can also result in single strand DNA nicks [26]. The results presented in this work suggest that neither neoamphimedine nor amphimedine produced significant double strand DNA breaks in cultured cells, consistent with *in vitro* cleavage data. It is likely that some DNA nicking occurs in neoamphimedine-treated cells, but this damage did not significantly contribute to the cytotoxicity of neoamphimedine in the xrs-6 cells. Therefore, it was hypothesized that neoamphimedine is a top2-dependent drug, whose primary mechanism of action is not the stabilization of cleavable complexes.

Cytotoxicity studies determined the relative potencies of neoamphimedine and amphimedine. While neoamphimedine was toxic in all tumor lines tested, its regioisomer was not. Further, it was determined that neoamphimedine is not a substrate for pg170 multi-drug resistance because it is equally toxic to both A2780 and MDR-expressing A2780AD cell lines.

All currently used clinical top2 poisons act, in part, by stabilizing cleavable complexes. This shared mechanism may limit the utility of these drugs. The primary top2-mediated effects on DNA by neoamphimedine were found to differ from clinical top2 poisons. Neoamphimedine induces top2-mediated catenation of plasmid DNA *in vitro*. Few molecules are known to induce mammalian top2 to catenate DNA. Spermidine, polyethylene glycol, PVA, histones and histone-like proteins carry this rare distinction [10,11,25,27–30]. These molecules require high concentrations to induce catenation, or are too large to make them viable drug candidates. In these systems, top2–DNA catenation is thought to be facilitated by neutralization of DNA charge, or by producing conditions that allow the compaction of DNA [30]. Neoamphimedine is a small, uncharged molecule, and it differs from its regioisomer and other pyridoacridines in only minor ways. However, we hypothesize that these minor changes significantly and uniquely affect its DNA interactions.

Neoamphimedine, at low concentrations, induces top2 to catenate DNA. Agarose gel, DNA filter binding and TEM analyses confirm this effect. DNA filter-binding assays also provide evidence that neoamphimedine facil-

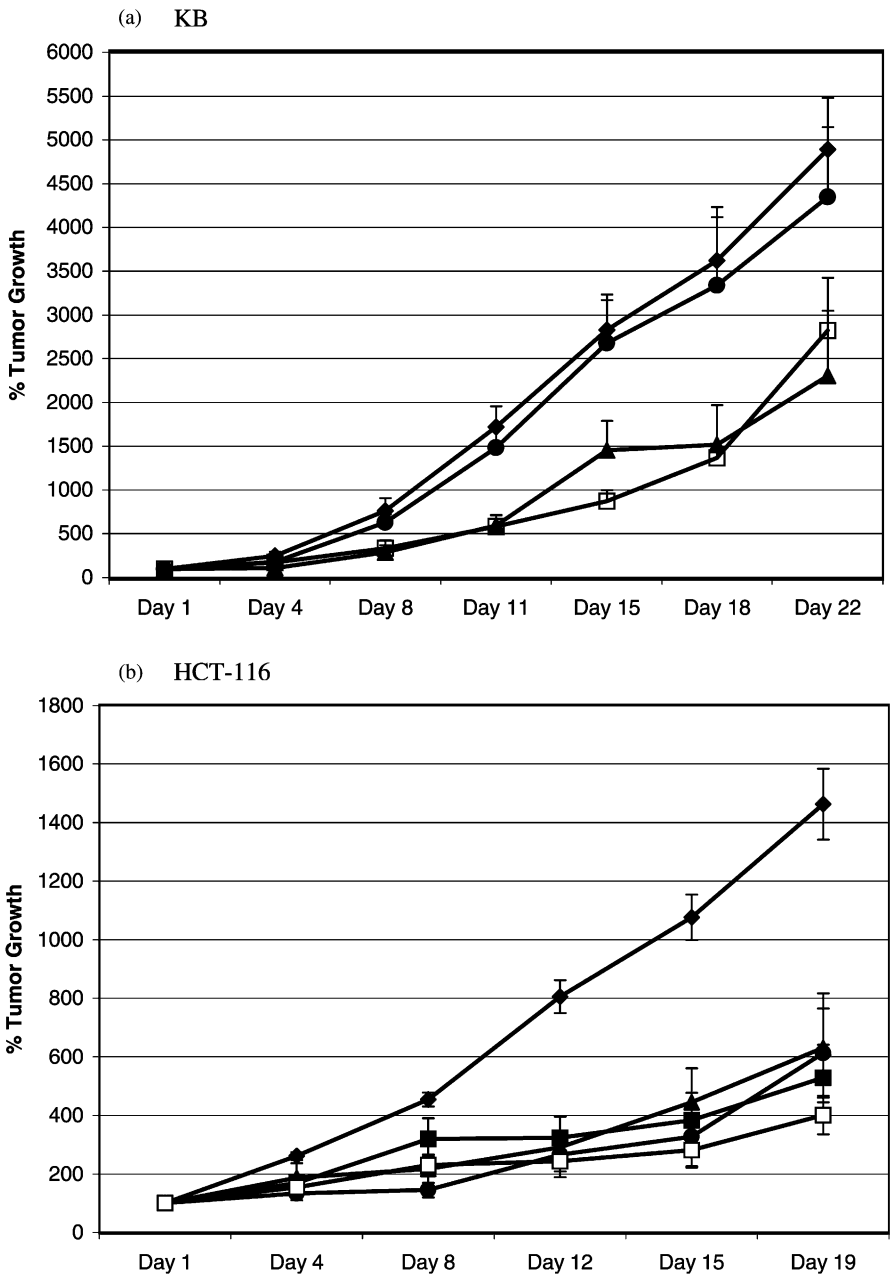

Fig. 7. *In vivo* activity of neoamphimedine in human epidermoid-nasopharyngeal and colon tumors. Human tumors grown in nude mice were tested to determine anti-neoplastic potential. (a) Neoamphimedine at 50 mg/kg (▲), amphimedine at 50 mg/kg (●), and etoposide at 50 mg/kg (□) were compared to control (◆) in KB cell line tumors. Significant difference ($P < 0.05$) was obtained by 50 mg/kg neoamphimedine on days 4, 8, 11, 15, 18, and 22; by 50 mg/kg etoposide on days 8, 11, 15, 18, and 22. There was no significant difference between amphimedine and control or neoamphimedine and etoposide. (b) 9-Aminocamptothecin at 1 mg/kg (□), neoamphimedine at 12.5 mg/kg (■), neoamphimedine at 25 mg/kg (●), and neoamphimedine at 50 mg/kg (▲) were compared to control (◆) in HCT-116 cell line tumors. Significant difference ($P < 0.05$) was obtained by 1 mg/kg 9-aminocamptothecin on days 8, 12, 15, and 19; by 12.5 mg/kg neoamphimedine on day 15, by 25 mg/kg neoamphimedine on days 4, 8, 12, and 15; and by 50 mg/kg neoamphimedine on days 8 and 12. Statistical analysis was done using multiple Student's *t*-tests. Values are means ± standard error, $N \geq 5$.

itates top2 plasmid catenation *in vitro* through DNA aggregation. Reports in other systems have suggested that the state of DNA could serve as a limiting factor in catenation [20,31]. To determine whether the supercoiled state of the plasmid DNA was influencing neoamphimedine catenation, reactions were carried out using relaxed plasmid DNA as substrate. Results were similar to those obtained with reactions utilizing supercoiled DNA. Agarose gel analysis (Tables 2 and 3) also showed the ability of neoamphimedine to induce top2-mediated single strand DNA breaks. The nicking activity disappeared as both the top2 concentrations and percent-catenated DNA increased. Similar concentration limited effects have been reported for other topoisomerase poisons [24,32]. The results suggest the possibility of competing mechanisms of neoamphimedine–top2 interaction.

In vivo studies demonstrated that the cytotoxicity induced by neoamphimedine possesses significant antitumor activity. KB tumors respond well to top2 drugs, including doxorubicin and etoposide. Neoamphimedine had activity equivalent to etoposide in mice bearing KB tumors. The top2 inactive isomer, amphimedine, had no detectable antitumor activity in this system. In addition, the more difficult to treat HCT-116 tumors also responded well to neoamphimedine. There was no significant difference between neoamphimedine and 9-aminocamptothecin, a drug effective in this system.

Top2 is an important drug target [33–36]. Understanding its mechanism of strand passage is a topic of active research [36,37]. We speculate that neoamphimedine influences top2–DNA interactions in a way that results in inappropriate strand passage *in vitro*. This activity is likely in equilibrium with its other effects on top2 and DNA and is potentially responsible for the unusual cytotoxic and antitumor activity of neoamphimedine.

Acknowledgments

The authors wish to thank Dr. Kurt Albertine and Nancy Chandler at the Research Microscopy Core Facility, University of Utah, for their kind assistance with the transmission electron microscope and image display, Christopher D. Pond for helpful suggestions, and to Heidi Fain for maintaining the cultured mammalian cell lines. The authors wish to acknowledge the support of Sea Grant N.O.A.A. grant NA36RG0537, NIH grant RO1 CA36622, and the DAMD sub-contract 179929033.

References

[1] Tewey KM, Chen GL, Nelson EM, Liu LF. Intercalative antitumor drugs interfere with the breakage-reunion reaction of mammalian DNA topoisomerase II. J Biol Chem 1984;259:9182–7.

[2] Covey JM, Kohn KW, Kerrigan D, Tilchen EJ, Pommier Y. Topoisomerase II mediated DNA damage produced by 4′-(9-acridinylamino)-methanesulfan-*m*-anisidide and related acridines in L1210 cells and isolated nuclei: relation to cytotoxicity. Cancer Res 1998;48: 860–5.

[3] Calabresi P, Chabner BA. Chemotherapy of neoplastic diseases. In: Gilman AG, Rall TW, Nies AS, Taylor P, editors. Goodman and Gilman's: the pharmacological basis of therapeutics. New York: Pergamon Press; 1990. p. 1239–44.

[4] de Guzman FS, Carte B, Troupe N, Faulkner DJ, Harper MK, Concepcion GP, Mangalindan GC, Matsumoto SS, Barrows LR, Ireland CM. Neoamphimedine: a new pyridoacridine topoisomerase II inhibitor which catenates DNA. J Org Chem 1999;64:1400–2.

[5] Bonnard I, Bontemps N, Lahmy S, Banaigs B, Combaut G, Francisco C, Colson P, Houssier C, Waring MJ, Bailly C. Binding to DNA and cytotoxic evaluation of ascididemin, the major alkaloid from the Mediterranean ascidian *Cystodytes dellechiajei*. Anticancer Drug Des 1995;10:333–46.

[6] Burres NS, Sazesh S, Gunawardana GP, Clement JJ. Antitumor activity and nucleic acid binding properties of dercitin, a new alkaloid isolated from a marine *Dercitus* species sponge. Cancer Res 1989; 49:5267–74.

[7] Gunawardana GP, Koehn FE, Lee AY, Clardy J, He H, Faulkner DJ. Pyridoacridine alkaloids from deep-water marine sponges of the family Pachastrellidae: structure revision of dercitin and related compounds and correlation with the kuanoniamines. J Org Chem 1992;57:1523–6.

[8] Dassonneville L, Wattez N, Baldeyrou B, Mahieu C, Lansiaux A, Banaigs B, Bonnard I, Bailly C. Inhibition of topoisomerase II by the marine alkaloid ascididemin and induction of apoptosis in leukemia cells. Biochem Pharmacol 2000;60:527–37.

[9] McDonald LA, Eldredge GS, Barrows LR, Ireland CM. Inhibition of topoisomerase II catalytic activity by pyridoacridine alkaloids from a *Cystodytes* sp. ascidian: a mechanism for the apparent intercalator-induced inhibition of topoisomerase II. J Med Chem 1994;37:3819–27.

[10] Low RL, Kaguni JM, Kornberg A. Potent catenation of supercoiled and gapped DNA circles by topoisomerase I in the presence of a hydrophilic polymer. J Biol Chem 1984;259:4576–81.

[11] Holden JA, Rolfson DH, Wittwer CT. The distribution of immunoreactive topoisomerase II protein in human tissues and neoplasms. Oncol Res 1992;4:157–66.

[12] Englund PT. The replication of kinetoplast DNA networks in *Crithidia fasciculata*. Cell 1978;14:157–68.

[13] Matsumoto SS, Haughey HM, Schmehl DM, Venables DA, Ireland CM, Holden JA, Barrows LR. Makaluvamines vary in ability to induce dose-dependent DNA cleavage via topoisomerase II interaction. Anticancer Drugs 1999;10:39–45.

[14] Nitiss J, Wang JC. DNA topoisomerase-targeting antitumor drugs can be studied in yeast. Proc Natl Acad Sci USA 1988;85:7501–5.

[15] Nitiss JL, Liu YX, Harbury P, Jannatipour M, Wasserman R, Wang JC. Amsacrine and etoposide hypersensitivity of yeast cells overexpressing DNA topoisomerase II. Cancer Res 1992;52:4467–72.

[16] Ito H, Fukuda Y, Murata K, Kimura A. Transformation of intact yeast cells treated with alkali cations. J Bacteriol 1983;153:163–8.

[17] Holden JA, Rolfson DH, Wittwer CT. Human DNA topoisomerase II: evaluation of enzyme activity in normal and neoplastic tissues. Biochemistry 1990;29:2127–34.

[18] Ausubel FM, Brent R, Kingston RE, Moore DD, Seidman JG, Smith JA, Struhl K. Current protocols in molecular biology. New York: Wiley Interscience; 1991.

[19] Sambrook J, Fritsch EF, Maniatis T. Molecular cloning. Cold Spring Harbor, New York: Cold Spring Harbor Laboratory Press; 1989.

[20] Thresher RJ, Griffith JD. Intercalators promote the binding of RecA protein to double-stranded DNA. Proc Natl Acad Sci USA 1990; 87:5056–60.

[21] Mosmann T. Rapid colorimetric assay for cellular growth and survival: application to proliferation and cytotoxicity assays. J Immunol Methods 1983;65:55–63.

[22] Denizot F, Lang R. Rapid colorimetric assay for cell growth and survival. Modifications to the tetrazolium dye procedure giving improved sensitivity and reliability. J Immunol Methods 1986;89:271–7.

[23] Jeggo PA, Caldecott K, Pidsley S, Banks GR. Sensitivity of Chinese hamster ovary mutants defective in DNA double strand break repair to topoisomerase II inhibitors. Cancer Res 1989;49:7057–63.

[24] Kokoshka JM, Capson TL, Holden JA, Ireland CM, Barrows LR. Differences in the topoisomerase I cleavage complexes formed by camptothecin and wakayin a DNA-intercalating marine natural product. Anticancer Drugs 1996;7:758–65.

[25] Holden JA, Low RL. Characterization of potent catenation activity of HeLa cell nuclei. J Biol Chem 1985;260:14491–7.

[26] Zechiedrich EL, Christiansen K, Andersen AH, Westergaard O, Osheroff N. Double-stranded DNA cleavage/religation reaction of eukaryotic topoisomerase II: evidence for a nicked DNA intermediate. Biochemistry 1989;28:6229–36.

[27] Liu LF, Depew RE, Wang JC. Knotted single-stranded DNA rings: a novel topological isomer of circular single-stranded DNA formed by

treatment with *Escherichia coli* omega protein. J Mol Biol 1976; 106:439–52.

[28] Tse Y, Wang JC. *E. coli* and *M. luteus* DNA topoisomerase I can catalyze catenation of decatenation of double-stranded DNA rings. Cell 1980;22:269–76.

[29] Brown PO, Cozzarelli NR. Catenation and knotting of duplex DNA by type 1 topoisomerases: a mechanistic parallel with type 2 topoisomerases. Proc Natl Acad Sci USA 1981;78:843–7.

[30] Krasnow MA, Cozzarelli NR. Catenation of DNA rings by topoisomerases. Mechanism of control by spermidine. J Biol Chem 1982; 257:2687–93.

[31] Rauch CA, Perez-Morga D, Cozzarelli NR, Englund PT. The absence of supercoiling in kinetoplast DNA minicircles. EMBO J 1993;12: 403–11.

[32] Larsen AK, Grondard L, Couprie J, Desoize B, Comoe L, Jardillier JC, Riou JF. The antileukemic alkaloid fagaronine is an inhibitor of DNA topoisomerase I and II. Biochem Pharmacol 1993;46:1403–12.

[33] Holden JA. DNA topoisomerases as anticancer drug targets: from the laboratory to the clinic. Curr Med Chem 2001;1:1–25.

[34] Froelich-Ammon SJ, Osheroff N. Topoisomerase poisons: harnessing the dark side of enzyme mechanism. J Biol Chem 1995;270:21429–32.

[35] Chen AY, Liu LF. DNA topoisomerases: essential enzymes and lethal targets. Annu Rev Pharmacol Toxicol 1994;34:191–218.

[36] Baird CL, Gordon MS, Andrenyak DM, Marecek JF, Lindsley JE. The ATPase reaction cycle of yeast DNA topoisomerase II. J Biol Chem 2001;276:27893–8.

[37] Lindsley JE. Use of a real-time, coupled assay to measure the ATPase activity of DNA topoisomerase II. Methods Mol Biol 2001;95:57–64.